Fatigue Growth of Surface Cracks in Notched Round Bars

Andrea Carpinteri, Roberto Brighenti, Andrea Spagnoli and Sabrina Vantadori

Department of Civil and Environmental Engineering & Architecture
University of Parma - Parco Area delle Scienze 181/A – 43100 Parma – Italy
E-mail: andrea.carpinteri@unipr.it

ABSTRACT. *A notch in a structural component can easily provoke the initiation and growth of a surface crack because of stress concentration. The stress field for this component can be rather different from that found out in an unnotched component with an identical surface flaw, and fatigue life may heavily be affected by such a geometric discontinuity. In the present paper, the influence of a circular-arc circumferential notch in a round bar is analysed. Firstly, the Stress Concentration Factor (SCF) related to tension loading is determined. Then, an elliptical-arc external surface flaw is assumed to exist at the notch root, and the Stress Intensity Factor (SIF) along the crack front is computed through a finite element analysis for both tension and bending, by varying the stress concentration factor from 1.0 (smooth bar) to about 3.0 (small notch radius). The effect of the stress concentration on the SIF values is discussed for the considered crack configurations. Finally, the surface crack propagation under cyclic loading is examined through a numerical procedure which takes into account the computed SIF values.*

INTRODUCTION

The presence of a notch in a structural component is a common occurrence in engineering practice, and can easily provoke the initiation and growth of a surface crack because of stress concentration [1-3]. In this case, the stress field can be rather different from that found out in an unnotched component with an identical surface flaw. Furthermore, fatigue life may heavily be affected by such a geometric discontinuity. For this reason, strength and fatigue life of structural components should be determined by taking into account the notch effect.

Several studies have been carried out in order to examine the influence of surface cracks in smooth components such as round bars [4-8], pipes and shells [4,6,9-12], whereas a few papers analyse round bars [13,14] and pipes [15,16] with hoop grooves.

In the present paper, a round bar with a circular-arc circumferential notch in the mid-length cross-section is considered. An elliptical-arc surface crack is assumed to exist in the notched (reduced) cross-section of the bar. The dimensionless Stress Intensity Factors (SIFs) for both tension (F) and bending about the normal to the symmetry notched cross-section axis (M_X) are determined through a finite element analysis, by varying the Stress Concentration Factor (SCF), K_t, from 1.0 (smooth bar) to about 3.0 (bar with a small notch radius), where the SCF is related to the tension loading case.

The effect of the stress gradient caused by the above notch on fracture and fatigue behaviour is evaluated for the bar being examined. In particular, fatigue crack paths (crack aspect ratio against relative crack depth) are determined through a numerical procedure based on a two-parameter theoretical model [7].

GEOMETRY AND LOADING CONDITIONS

The round bar being considered presents a circumferential notch characterized by a constant curvature radius ρ and a depth c (Fig. 1), with a transversal surface crack at the notch root. The diameter of the bar is equal to D_0 and D in an unnotched cross-section and in the notched cross-section, respectively. The relative notch radius and the relative notch depth are defined as $\rho_d = \rho / D_0$ and $\delta = c / D_0$, respectively. In the following, the relative notch depth δ is assumed to be equal to 0.1 for each value of the notch radius (i.e. $D = 0.8 D_0$). The bar is subjected to both tension (F) and bending about the normal to the symmetry notched cross-section axis (M_X).

For each value of ρ_d, a stress concentration factor value is obtained, as is described below. Note that, for a given notched geometry, the SCF K_t (taken as the ratio between
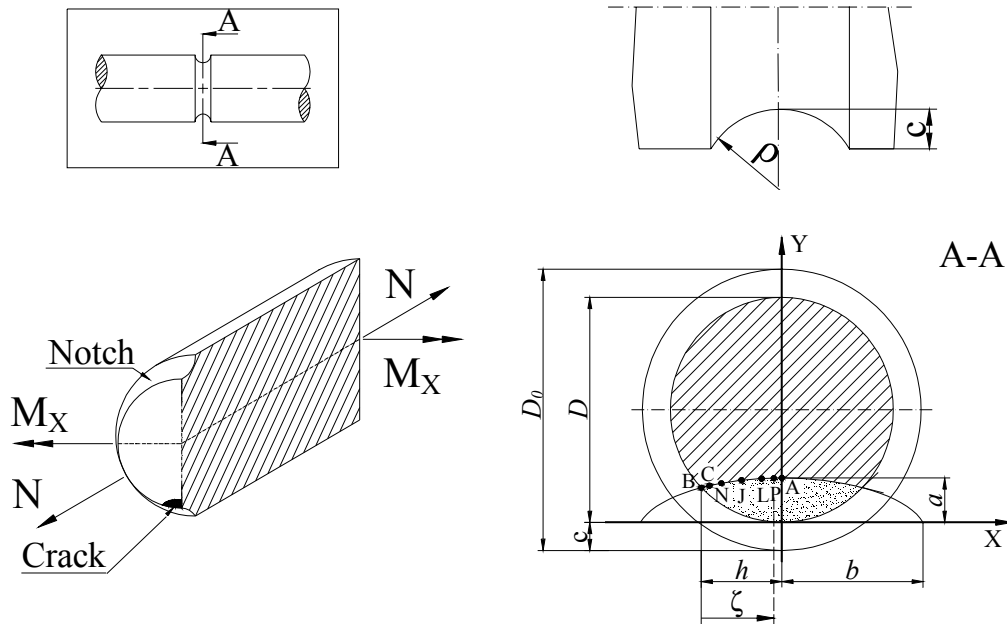
Figure 1. Notched bar with a surface crack: geometry and loading conditions.

the maximum stress and the corresponding nominal stress in the notched cross-section) is univocally related to the loading condition applied. An axisymmetric finite element analysis with an increasing number of elements (h-convergence test) has been carried out in order to obtain the asymptotic K_t values for uncracked notched bars under tension. The relative notch radius ρ_d has been assumed to be equal to 0.1, 0.2, 0.5, 0.7 (blunt notch) and ∞ (unnotched bar), where such notch configurations correspond to K_t values equal to about 2.83, 2.19, 1.70, 1.58 and 1.0 in the case of tension loading.

Then, an external surface crack is assumed to exist in the notched cross-section of the structural component. Such a flaw presents an elliptical-arc shape (Fig.1). The crack configuration being examined is described by the relative crack depth $\xi = a / D$ of the deepest point A on the defect front (with $0.1 \leq \xi \leq 0.8$), and the flaw aspect ratio $\alpha = a / b$ (with $0 \leq \alpha \leq 1.2$), whereas the generic point P along the crack front is identified by the dimensionless coordinate $\zeta^* = \zeta / h$ (Fig.1).

STRESS INTENSITY FACTOR EVALUATION

A finite element model has been adopted to determine the SIF values along the crack front. Due to the symmetry of the problem, only a quarter of the bar has been modelled by 20-node isoparametric finite elements. Quarter-point wedge finite elements have been used along the crack front in order to model the stress field singularity. A total number of 3186 finite elements and 14367 nodes have been employed. The SIF values have been obtained from the displacements of the wedge finite elements, measured in correspondence to the quarter-point nodes.

Dimensionless SIFs, normalised with respect to the reference stresses σ_F and σ_{M_X} for tension and bending, respectively, are defined as follows:

$$K^*_{I,F} = \frac{K_{I,F}}{\sigma_F \sqrt{\pi a}} \qquad\qquad K^*_{I,M_X} = \frac{K_{I,M_X}}{\sigma_{M_X} \sqrt{\pi a}} \qquad (1)$$

where

$$\sigma_F = \frac{4 F}{\pi D_0^2} \qquad\qquad \sigma_{M_X} = \frac{32 M_X}{\pi D_0^3} \qquad (2)$$

The K_t parameter is very important especially in presence of cracks, since it heavily affects the SIF results. The dimensionless SIFs along the crack front, determined through the above finite element analysis, are displayed for both tension and bending loading in Figs 2 and 3, respectively, for K_t values equal to 2.83 $(\rho_d = 0.1)$ and 1.0 $(\rho_d = \infty)$. Different values of ξ and α are considered. The effect of the stress concentration on the SIFs can be observed. For instance, the dimensionless SIFs for $\rho_d = 0.1$ are greater than those for $\rho_d = \infty$, the values of the other parameters being the
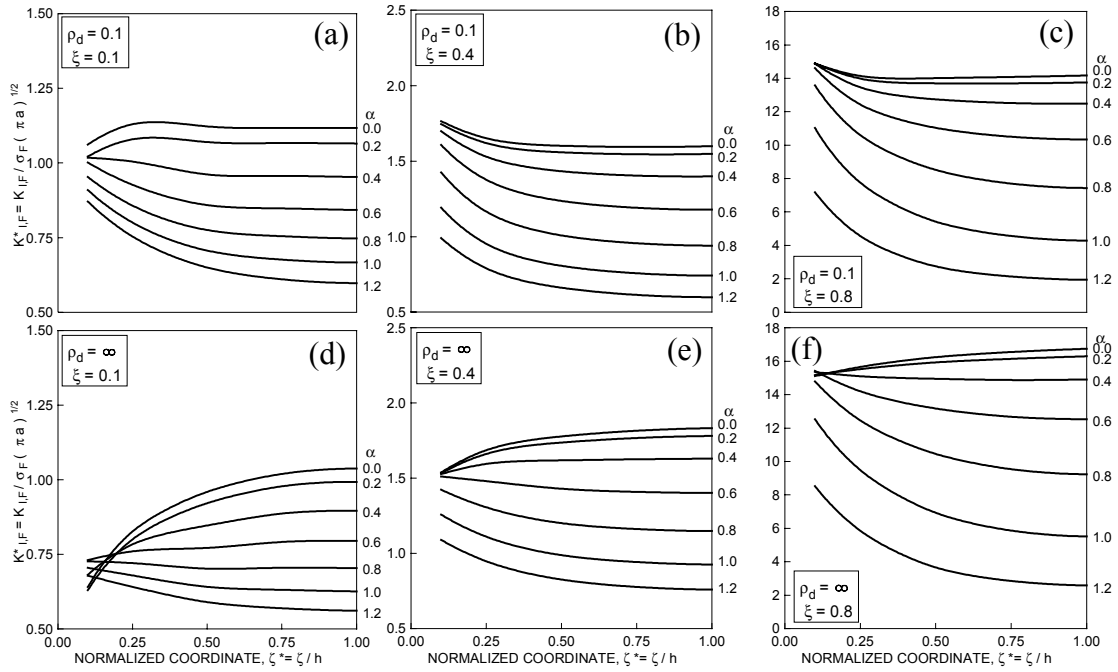
Figure 2. Dimensionless SIF $K_{I,F}^*$ along the crack front (ζ^*), for different values of α: $K_t = 2.83$ ($\xi = 0.1$ (a), $\xi = 0.4$ (b), $\xi = 0.8$ (c)); $K_t = 1.00$ (unnotched bar) ($\xi = 0.1$ (d), $\xi = 0.4$ (e), $\xi = 0.8$ (f)).
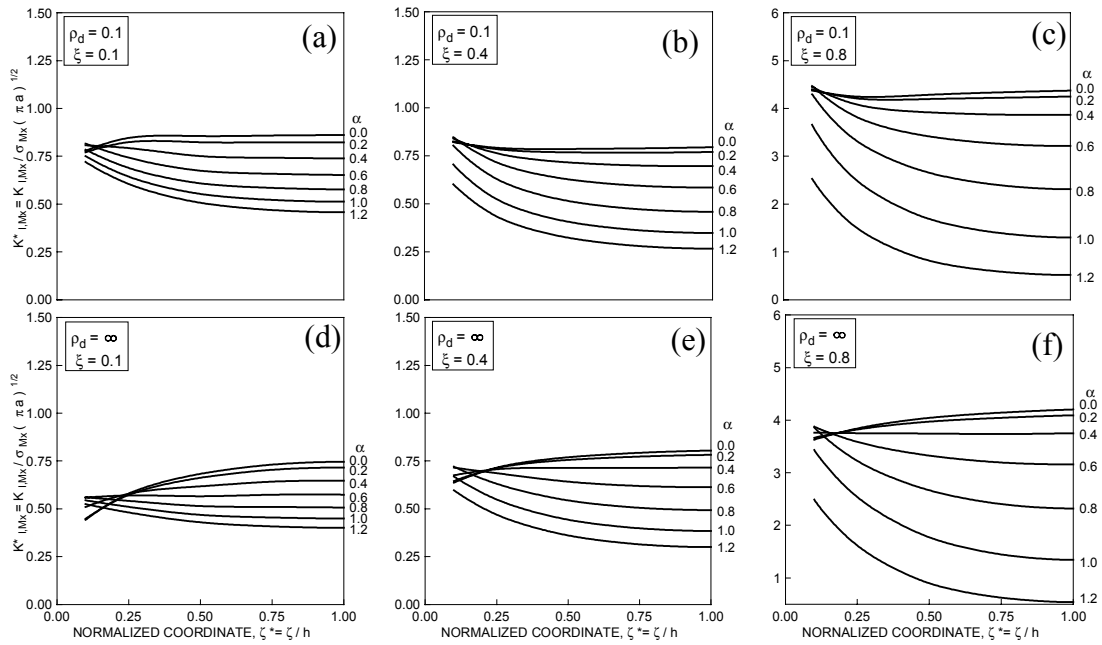
Figure 3. Dimensionless SIF $K_{I,M}^*$ along the crack front (ζ^*), for different values of α: $K_t = 2.83$ ($\xi = 0.1$ (a), $\xi = 0.4$ (b), $\xi = 0.8$ (c)); $K_t = 1.00$ (unnotched bar) ($\xi = 0.1$ (d), $\xi = 0.4$ (e), $\xi = 0.8$ (f)).

same, that is, the SIFs tend to increase because of the notch presence. Such an increase varies with the crack geometry. The maximum value of SIF, along the crack front, is attained at either the deepest point (A) or the near-surface point (C), depending on the values of both ξ and α .

The dimensionless SIFs for both tension and bending are shown against K_t in Fig. 4, for different crack configurations. It can be noted that, depending on both crack geometry and loading conditions, SIF values may either increase, or decrease or have a non-monotonic trend with increasing K_t, the values of the other parameters being the same.
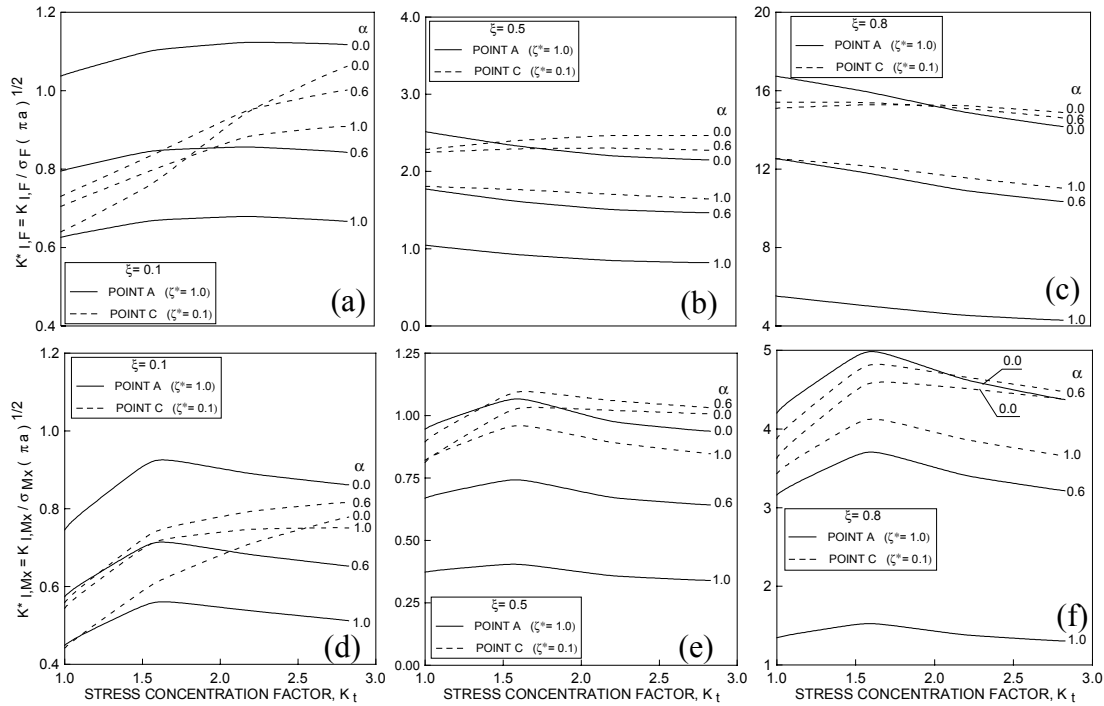
Figure 4. Dimensionless SIF vs SCF at point A and point C on the crack front:
(a) to (c) tension; (d) to (f) bending.

FATIGUE CRACK GROWTH

Now the fatigue propagation paths of the above surface flaws in notched bars under tension or bending loading are determined by applying a two-parameter theoretical model [7]. According to such a model, the crack front lying on an ellipse with semi-axes a and b grows after one cyclic loading step to a new configuration described by the following equation :

$$\frac{x^2}{(b^*)^2} + \frac{y^2}{(a^*)^2} = 1 \tag{3}$$

where the two unknowns a^* and b^* (semi-axes of the new crack front) can be deduced through the condition that the coordinates of the new points A* and C*, obtained from those of the old points A and C by employing the Paris-Erdogan law, must satisfy Eq.(3). Details of this procedure can be found elsewhere [7]. In the following examples, the material constants Q and m of the fatigue law ($da/dN = Q(\Delta K_I)^m$, with da/dN in mm cycle^{-1} and the SIF range ΔK_I in N mm$^{-3/2}$) are assumed to be equal to 1.64×10^{-10} and 2, respectively. The axial force (F) and the bending moment (M_X) are made to vary from zero to a maximum value in each fatigue loading cycle, so that $\Delta\sigma_F = \Delta\sigma_{M_X} = 100$ MPa.

The curves of crack aspect ratio against relative crack depth are shown in Fig. 5 for tension (Fig 5a-b) and bending (Fig. 5c-d), in the case of notched ($\rho_d = 0.1$) and unnotched ($\rho_d = \infty$) bars. It can be noted that, for notched bars, the crack front tends to become straight as the crack depth increases. On the other hand, for unnotched bars, the $\alpha - \xi$ curves approach an inclined asymptote with increasing ξ. Results from some
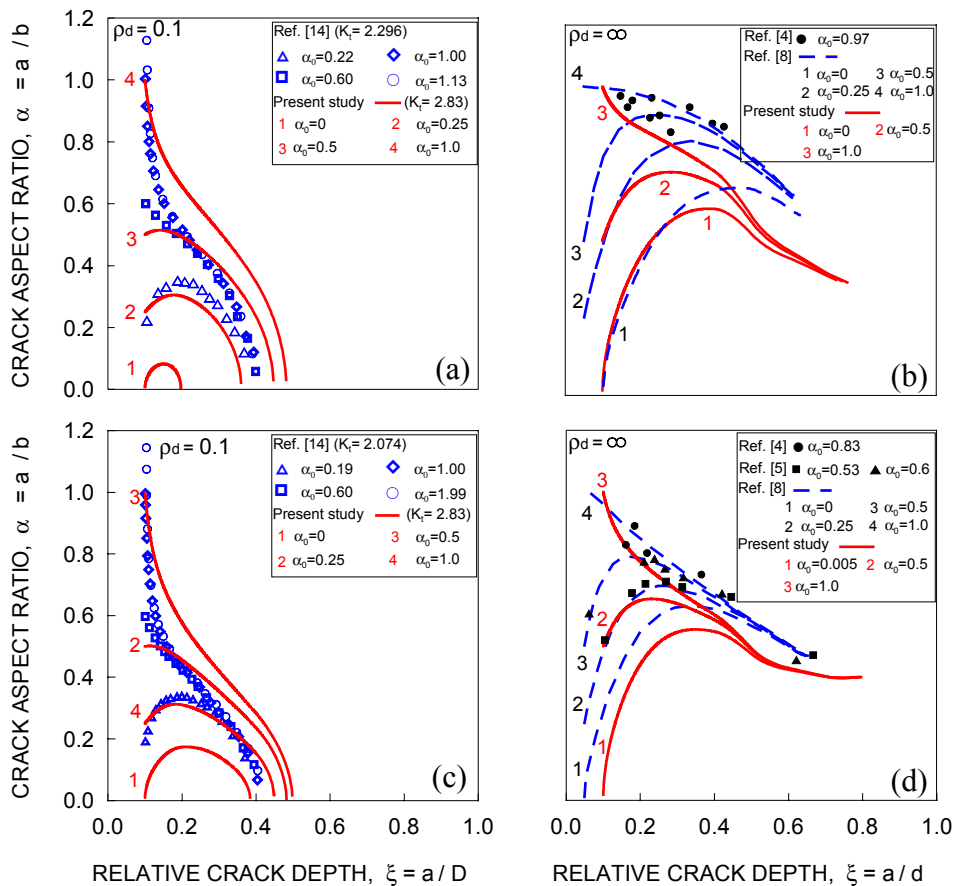
Figure 5. Crack aspect ratio vs relative crack depth curves for notched ($\rho_d = 0.1$) and unnotched ($\rho_d = \infty$) bars : (a) to (b) tension; (c) to (d) bending.

relevant numerical investigations [4,5,8,14] are also reported in Fig. 5. The comparison between the results shown is fairly satisfactory, also considering that the initial crack configurations and the notch geometries in the present study are slightly different from those of the other investigations being examined.

Finally, the shape evolution of the crack front for both tension and bending at different numbers of fatigue loading cycles is displayed in Fig. 6, by juxtaposing the results for notched ($\rho_d = 0.1$, dashed line) and unnotched ($\rho_d = \infty$, continuous line) bars. The numbers near the crack fronts indicate the thousands of loading cycles to reach the various flaw configurations.
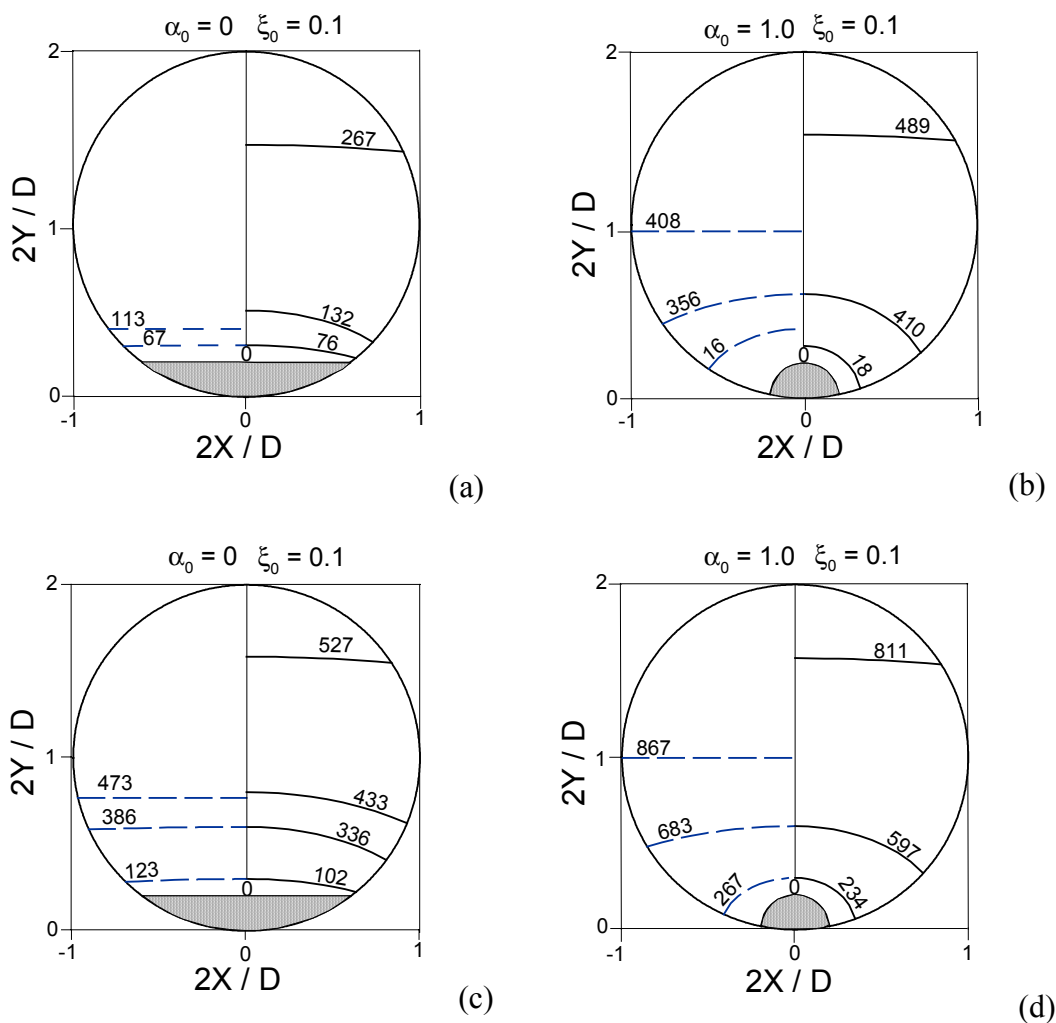
Figure 6. Shape evolution of the crack front (only half crack front is reported), for initially straight ($\alpha_0 = 0$, see (a) and (c)) and circular ($\alpha_0 = 1$, see (b) and (d)) fronts, at different numbers of fatigue loading cycles, for notched ($\rho_d = 0.1$, dashed line) and unnotched ($\rho_d = \infty$, continuous line) bars : (a) to (b) tension; (c) to (d) bending.

CONCLUSIONS

The behaviour of a notched round bar with a part-through crack under both tension and bending has been examined. The circumferential notch is assumed to have a circular-arc shape, whereas the surface flaw at the notch root presents an elliptical-arc shape.

First of all, the Stress Concentration Factor (SCF) due to the circumferential groove has been computed for the tension loading case. Then, in order to obtain the Stress Intensity Factor (SIF) distribution for different values of the SCF and crack geometries, a finite element analysis has been performed.

The notch effect on the SIF has been determined to be significant for any crack size and shape. Insofar as fatigue behaviour is concerned, a remarkable influence of the stress field caused by the notch is demonstrated. The comparison between the crack aspect ratio vs relative crack depth curves of the present study and those by other authors appears satisfactory.

ACKNOWLEDGEMENTS

REFERENCES

1. Pook, L.P. (1983) *The Role of Crack Growth in Metal Fatigue*. Metals Society, London.
2. Carpinteri, A. (Ed.) (1994) *Handbook of Fatigue Crack Propagation in Metallic Structures*. Elsevier Science BV, Amsterdam.
3. Pook, L.P. (2002) *Crack Paths*. WIT Press, Southampton.
4. Forman, R.G. and Shivakumar, V. (1986) *Fract. Mech.* **30**, 59-74.
5. Lorentzen, T., Kjaer, N.E. and Henriksen, T.K. (1986) *Engng Fract. Mech.* **23**, 1005-1014.
6. Raju, I.S. and Newman, J.C. Jr. (1986). In: *Fract. Mech. 17th Volume*, pp.789-805, ASTM STP 905.
7. Carpinteri, A. (1993) *Int. J. Fatigue* **15**, 21-26.
8. Carpinteri, A. and Brighenti, R. (1996) *Int. J. Fatigue* **18**, 33-39.
9. Bergman, M. (1995) *Fatigue Fract. Engng Mater. Struct.* **18**, 1155-1172.
10. Lin, X.B. and Smith, R.A. (1997) *Int. J. Pres. Ves. & Piping* **71**, 293-300.
11. Carpinteri, A., Brighenti, R. and Spagnoli, A. (1998) *Nuclear Engng Design* **185**, 1-10.
12. Carpinteri, A., Brighenti, R. and Spagnoli, A. (2000) *Fatigue Fract. Engng Mater. Struct.* **23**, 467-476.
13. Lin, X.B. and Smith, R.A. (1998) *Int. J. Mech. Sci.* **40**, 405-419.
14. Lin, X.B. and Smith, R.A. (1999) *Int. J. Fatigue* **21**, 965-973.
15. Zhang, Q.Y. and Liu, Y. (1992) *Int. J. Pres. Ves. & Piping* **51**, 361-372.
16. Liu, Y., Zhou, S.S. and Cai, Sh.T. (1993) *Int. J. Pres. Ves. & Piping* **53**, 393-404.